The HARPS search for southern extra-solar planets[*]

XVIII. An Earth-mass planet in the GJ 581 planetary system

M. Mayor[1], X. Bonfils[2,3], T. Forveille[2], X. Delfosse[2], S. Udry[1], J.-L. Bertaux[4], H. Beust[2], F. Bouchy[5], C. Lovis[1], F. Pepe[1], C. Perrier[2], D. Queloz[1], and N. C. Santos[1,6]

[1] Observatoire de Genève, Université de Genève, 51 ch. des Maillettes, CH-1290 Sauverny, Switzerland e-mail: `michel.mayor@obs.unige.ch`
[2] Laboratoire d'Astrophysique, Observatoire de Grenoble, Université J.Fourier, CNRS (UMR5571), BP 53, F-38041 Grenoble, Cedex 9, France
[3] Centro de Astronomia e Astrofísica da Universidade de Lisboa, Observatório Astronómico de Lisboa, Tapada da Ajuda, 1349-018 Lisboa, Portugal
[4] Service d'Aéronomie du CNRS, BP 3, 91371 Verrières-le-Buisson, France
[5] Institut d'Astrophysique de Paris, CNRS, Université Pierre et Marie Curie, 98bis Bd Arago, 75014 Paris, France
[6] Centro de Astrofísica, Universidade do Porto, Rua das Estrelas, P4150-762 Porto, Portugal

ABSTRACT

The GJ 581 planetary system was already known to harbour three planets, including two super-Earths planets which straddle its habitable zone. We report here the detection of an additional planet – GJ 581e – with a minimum mass of 1.9 $M_\oplus$. With a period of 3.15 days, it is the innermost planet of the system and has a ∼5% transit probability.

We also correct our previous confusion of the orbital period of GJ 581d (the outermost planet) with a one-year alias, thanks to an extended time span and many more measurements. The revised period is 66.8 days, and locates the semi-major axis inside the habitable zone of the low mass star.

The dynamical stability of the 4-planet system imposes an upper bound on the orbital plane inclination. The planets cannot be more massive than approximately 1.6 times their minimum mass.

Key words. stars: individual: GJ 581 – stars: planetary systems – stars: late-type – technique: radial-velocity

1. Introduction

HARPS is a vacuum spectrograph designed to measure precise radial velocities, with the specific goal of searching for exoplanets in the Southern hemisphere Mayor et al. (2003). This high-resolution Echelle spectrograph (R=115000) is fiber-fed by the ESO 3.6-meter telescope at La Silla Observatory. The consortium which built this instrument was granted 500 observing nights over five years to conduct a comprehensive search for exoplanets. This large programme addresses several key exoplanet questions, including the characterization of very low mass exoplanets. A significant fraction of the observing time was devoted to the study of planets orbiting stars at the bottom of the main sequence. The M-dwarf sub-programme includes over 100 stars, which form a volume-limited sample.

Our HARPS search for southern exoplanets orbiting M-dwarfs is on-going, and has been recently expanded to a larger sample of some 300 low-mass stars. Several planets have already been detected in the M-dwarf survey: GJ 581 b (Bonfils et al. 2005b), GJ 581 c and d (Udry et al. 2007), GJ 674 (Bonfils

et al. 2007), GJ 176 (Forveille et al. 2009), and here a fourth planet in the GJ 581 system. These 6 planets all have minimum masses under approximately 15 Earth-masses. They represent approximately half of the known inventory of planets orbiting M stars, and most of its lowest mass members. Besides the HARPS planets, this inventory includes three planets around GJ 876 (Delfosse et al. 1998; Marcy et al. 1998, 2001; Rivera et al. 2005), a single Neptune-mass planet orbiting GJ 436 (Butler et al. 2004), jovian planets bound to GJ 849 (Butler et al. 2006) and to GJ 317 (Johnson et al. 2007), and finally a gaseous giant planet orbiting GJ 832 (Bailey et al. 2009). Altogether, 8 planetary systems centered on M dwarfs have been identified by the radial velocity technique, for a total of 12 planets. Although the statistics are still limited, and come from surveys with different sensitivities, they indicate that multi-planet systems are common: the fraction of known multiple systems around M dwarfs is already 2/8 (25%), and it reaches 5/8 (63%) if one accounts for systems where a radial velocity drift indicates an additional long-period planet.

The competing teams which monitor M dwarfs with Doppler spectroscopy have together observed over 300 stars for several years. Planetary systems with at least one identified gaseous giant planet have been found around ∼1.5% of these low mass stars, and that proportion is clearly lower than for K and G dwarfs. Up to periods of several hundred days this comparative deficit of Jupiter-mass planets for M dwarfs is statistically robust (Bonfils et al. 2006; Endl et al. 2006; Johnson et al. 2007).

Send offprint requests to: M. Mayor

Conversely, planets less massive than ~25 $M_\oplus$ are significantly more frequent around M dwarfs (Bonfils et al. 2007, and 2009 in preparation).

The GJ 581 system is of particular interest, as two of its previously detected planets are located on the two edges of the habitable zone (HZ) of the M3V host star (Selsis et al. 2007; von Bloh et al. 2007). Despite the uncertainties on the exact location of the "liquid water" zone for planets more massive than the Earth, these detections demonstrate that super-Earths in the HZ can be detected by Doppler spectroscopy, for planets orbiting M dwarfs.

In the present paper, we report the detection of a fourth planet in the GJ 581 system, 'e', with a minimum mass of 1.94 $M_\oplus$. We also correct the period of the outer planet GJ 581d, and find that the revised period locates GJ 581d in the habitable zone. In Section 2 we briefly recall the main characteristics of the host star GJ 581, and of its first three planets. An enlarged set of measurements (Section 3) allows a reexamination of the structure of the GJ581 planetary system, and the discovery of an additional very-low-mass planet (Section 4). Since Doppler spectroscopy, and all the more so for M dwarfs, can be confused by stellar surface inhomogeneities, we dedicate Section 5 to discussing the magnetic activity of GJ 581. In Section 6, we use dynamical stability considerations to obtain upper limits to the planetary masses. To conclude, we briefly discuss how this system meshes up with theoretical predictions, and consider the prospects of finding even lower mass planets in the habitable zone of M dwarfs.

2. Stellar caracteristics and planetary system

Our report of the first Neptune-mass planet on a 5.36-d orbit around GJ 581 (Bonfils et al. 2005b) extensively describes the properties of the host star. Here we will therefore only summarize those characteristics.

GJ 581 (HIP 74995, LHS 394) is an M3 dwarf at a distance to the Sun of 6.3 pc. Its estimated luminosity is only 0.013 $L_\odot$. Bonfils et al. (2005a) find GJ 581 slightly metal-poor ([Fe/H] = -0.25), in contrast to the supersolar metallicities (Santos et al. 2001, 2004) of most solar-type stars hosting giant planets. All indirect tracers (kinematics, stellar rotation, X-ray luminosity, and chromospheric activity) suggest a minimum age of 2 Gyr. The HARPS spectra show weak Ca II H and K emission, in the lower quartile of stars with similar spectral types. This very weak chromospheric emission points towards a long stellar rotation period.

The first planet was easily detected after only 20 HARPS observations (Bonfils et al. 2005b), and the periodogram of the residuals of that first solution hinted at power excess around 13 days. As 30 additional observations were accumulated for a total time span of 1050 days, that coherent signal strengthened to strong significance, and a third planet appeared, though still with a significant False Alarm Probability (FAP): GJ 581c had $m \sin i = 5M_\oplus$, $P = 12.9$ days) and a ~ 0.28% FAP, while the more distant GJ 581d had $m \sin i = 7.7M_\oplus$, $P = 83$ days, and a ~ 3% FAP. (Udry et al. 2007). Udry et al. (2007) therefore ended on a call for confirmation by additional radial velocity measurements, and based on the very-low magnetic activity of GJ 581, suggested that the significant residuals might reflect additional planets in the system.

3. A new data set

Following up on that call for more data, we have now recorded a total of 119 HARPS measurements of GJ 581 (Table 1, only available electronically), which together span 1570 days (4.3 years). In parallel to this extension of the data set, the precision of all measurements, including the previously published ones, has been improved. The reference wavelengths of the thorium and argon lines of the calibration lamps were revised by Lovis & Pepe (2007), and most recently Lovis (2009, in prep.) implemented a correction for the small effect of Th-Ar calibration lamp aging. The changing internal pressure of aging lamps shifts the wavelength of their atomic transition. The effect is now corrected down to a level of just a few 0.1 m/s, using the differential pressure sensitivity of the argon and thorium lines. The HARPS pipeline also corrects the radial velocities to the Solar System Barycentric reference frame (Lindegren & Dravins 2003). That correction is computed at the weighted-mean time of the exposure, which is measured by a photometer that diverts a small fraction of the stellar flux. This effective time of the exposure is measured to better than 1%, which at the latitude of La Silla Observatory and for 900s-long exposures translates into a ~ 0.3 m s^{-1} worst case error on the Earth-motion correction. The combined photon noise, calibration error, and error on the mean time of the exposure result in a typical overall uncertainty of 1 m s^{-1}, with a full range of 0.7 to 2 m s^{-1} which reflects the weather conditions. Finally, the pipeline corrects for the 0.20 m s^{-1} yr^{-1} perspective acceleration from the proper motion of the star (e.g. Kürster et al. 2003).

4. GJ 581, a system with four low-mass planets

Our preferred method for planet searches in RV data uses a heuristic algorithm, which mixes standard non-linear minimizations with genetic algorithms. It efficiently explores the large parameter space of multi-planet systems, and quickly converges toward the best solution. We tried models composed of zero to five planets on Keplerian orbits, and found that the data require a 4-planets model.

To verify the robustness of that 'black-box' solution, and gain insight on its content, we also performed a step by step periodogram analysis. The top panel of Fig. 1 displays the window function of our RV measurements, and unsurprisingly shows that the dominant periodicities of our sampling are 1 day and 1 year. The second panel is a floating-mean periodogram (Gilliland & Baliunas 1987; Zechmeister & Kürster 2009) of the RVs. It is dominated by a ~5.36-day periodicity, which corresponds to GJ 581b. To estimate the FAP of that peak, we generated virtual data sets using boostrap resampling (Press et al. 1992) of the actual measurements, and examined the peak power in the periodogram of each of these virtual datasets. None of 10,000 trials had as high a peak as measured for the actual 5.36-day signal, which therefore has a FAP below 0.01%. We then adjusted a Keplerian orbit with that starting period, and examined the periodogram of the residuals of this 1-planet solution (Fig. 1, 3rd panel). That second periodogran is dominated by a peak around ~ 12.9 day, with a FAP<0.01%, which corresponds to the known planet GJ 581c. We then investigated the periodogram of the residuals of the corresponding 2-planets least square adjustment. That new periodogram has power excess in the 50-90 days range and around 3.15 days (as well as at 1-day aliases of these periods), both with FAPs<0.01%. The broad power excess between 50 and 90 days splits into 3 separate peaks at ~59, 67 and 82 days, which are 1-year aliases of each other

$(1/67 - 1/365 \sim 1/82, 1/67 + 1/365 \sim 1/59,)$. In Udry et al. (2007), we attributed an 82-days period to GJ 581 d. The corresponding periodogram peak now has markedly less power than the 67-days periodicity, and attempts to adjust orbits with that period (as well as with a 59 days period) produced significantly larger residuals. We conclude that the actual period of GJ 581 d is around 67 days and that we had previously been confused by a 1-year alias of that period. As we discuss below, the revised period locates GJ 581 d in the habitable zone of GJ 581. Subtracting the corresponding 3-planet adjustement leaves no power excess in the 50-90 days range (5th panel), and markedly enhances the 3.15 day peak. The residuals of this 4-planet solution finally display no statistically significant peak (6th panel). The strongest peak is located close to one year ($P \sim 384$ day) and has a ~50% FAP.

Both the heuristic algorithm and the spectral analysis method find the same 4 coherent signals in our data. Once this best approximate 4-planet solution had been identified, we performed a final global least square adjustment, using the iterative Levenberg-Marquardt algorithm. Since we find insignificant eccentricities for planets 'b' and 'c', we fixed the eccentricities and longitude of periastron to zero for both planets. Table 2 lists the resulting orbital elements, and Fig. 2 displays the corresponding Keplerian orbits.

Compared to our Udry et al. (2007) study, we thus add a fourth planet and very significantly revise the characteristics of the outer planet (GJ 581d), and in particular its period. Planets b to e have respective minimum masses of $m \sin i \sim 15.7, 5.4, 7.1$ and $1.9\ M_{\oplus}$. GJ 581e is the lowest mass exoplanet detected so far around a main sequence star. None of the period ratios of the system comes close to any simple ratio of integers, with e.g. $P_b/P_e = 1.70$, $P_c/P_b = 2.4$ and $P_d/P_c = 5.17$. Non-resonant hierarchies have similarly been noticed for all multi-planet systems which only contain low mass planets, such as HD 40307 (Mayor et al. 2009) and HD 69830 (Lovis et al. 2006).

5. Planets rather than spots

Coherent Doppler shifts unfortunately do not always correspond to planets. Inhomogeneities of the stellar surface like spots, plages, flares or convective patterns can break the even distribution between the blue- and red-shifted halves of a rotating star and induce apparent radial velocity shifts. At best, this introduces noise on the RV measurements, which is usually referred to as "jitter". In some cases the surface pattern can be stable over long time spans (from days to years), and the "jitter" noise then is correlated. In such cases, it does not average out as white noise would, and instead builds up a coherent signal. That apparent Doppler shift can easily happen to mimic a Keplerian orbit (e.g. Queloz et al. 2001; Bonfils et al. 2007).

M dwarfs notoriously tend to have stronger magnetic activity than solar-like stars, and possible false detections from coherent jitter therefore need even closer scrutiny. We have indeed encountered several such cases in our M star survey, including GJ 674 (Bonfils et al. 2007) and GJ 176 (Forveille et al. 2009). In both cases, photometric monitoring and spectroscopic activity diagnostics (measuring the Ca II H&K and H$_\alpha$ lines) demonstrated that a seemingly Keplerian signal was in fact due to spot modulation of the absorption line profiles. These two examples serve as reminders that a periodic Doppler signal does not always reflect the presence of a planet, and that additional checks are needed to conclude.

In our previous papers on the GJ 581 system, we could exclude any such confusion for the first three planets. The ~

$13\,\mathrm{m\,s^{-1}}$ radial velocity amplitude due to GJ 581 b ($P = 5.36$ day – Bonfils et al. 2005b) is sufficiently large that a spot signal of that magnitude would have induced measurable distortions of the rotational profile. The lack of any correlation between the bisector span (a first order measurement of spectral lines asymmetry) and the measured RVs, excludes that scenario. The strength of the Ca II H&K emission lines in addition classifies GJ 581 in the lowest ~ 5% magnetic activity bin of our M dwarfs sample. This implies a much longer rotation period than the observed 5.4 days, as confirmed by the very low projected rotational velocity $v \sin i < 1$ km s^{-1}). That velocity would need an unprobably low inclination i to be compatible with a 5 days rotation period, The additional measurements since Bonfils et al. (2005b) have strengthened those conclusions even further.

In Udry et al. (2007), we used distinct lines of arguments for the 12.9 and the 83 days (now 67 days) signals. The arguments developed above for GJ 581b hold for the 12.9-day period, which is also too short to be compatible with the rotation period. They also apply for GJ 581e at 3.1 days. An 83 days (or 67 days) period, on the other hand, would be perfectly consistent with the rotation period of an M dwarf with the activity level of GJ 581. For such long periods the bisector span also loses its diagnostic power, because the rotational profile becomes much too narrow to resolve with HARPS. This calls for a different argument, and we used a relation by Saar & Donahue (1997) to estimate the minimum filling factor of a spot that could produce the observed radial velocity signal. That relation,

$$K_s \sim 6.5 \times f_s^{0.9} \times v \sin i \quad [\mathrm{m\,s^{-1}}] \tag{1}$$

connects the semi-amplitude K_s of the radial-velocity signal induced by an equatorial spot with its surface filling factor, $f_s\%$, and the projected rotation velocity, $v \sin i$. It has been validated in numerous examples, including e.g. GJ 674 and GJ 176. Applying that relation to a $R_\star = 0.31\ R_\odot$ stellar radius, a $P = 83$ days period and a $K \sim 2.5$ m s^{-1} semi-amplitude, Eq. (1) readily showed that the GJ 581 d signal would have needed a $f_s \sim 2.2\%$ filling factor to be explained by a spot. Such a large spot is firmly excluded by the sub-% photometric stability of GJ 581.

Our revised 66.7 days period for GJ 581 d slightly weakens that argument, since a shorter period signal can be induced by a smaller spot. The revision however is minor, as the 67-day signal still requires a $f_s = 1.7\%$ spot, which is easily excluded by the improved photometric measurements that have become available since Udry et al. (2007). The strongest photometric stability constraint is provided by 6 weeks of continuous monitoring of GJ 581 by the MOST satellite. Preliminary results, presented by J. Matthews at the 2007 Michelson Summer School[1], indicate that the peak-to-peak photometric variability during those 6 weeks was less than 5 mmag. The 66.7-day HARPS radial velocity signal is therefore incompatible with rotational modulation of spots or granulation patches.

The variations of the chromospheric Ca II H+K line (Table 1, only available electronically) provide another diagnostic of magnetic activity, which proved very valuable for GJ 674 (Bonfils et al. 2007). We parametrize this chromospheric emission by

$$Index = \frac{H + K}{R + B}, \tag{2}$$

where H (resp. K) is the flux measured in the Ca II H (resp. K) line and where R and B measure the flux in pseudo-continuum bands on both sides of the lines. Fig. 3 displays our Ca II H+K

---

[1] http://nexsci.caltech.edu/workshop/2007/Matthews.pdf

Table 2. Fitted orbital solution for the GJ 581 planetary system: 4 Keplerians. The model imposes circular orbits for planets GJ 581 b & e, since the derived eccentricities for a full Keplerian solution are insignificant (see text).

Parameter		GJ 581 e	GJ 581 b	GJ 581 c	GJ 581 d
P	[days]	3.14942 ± 0.00045	5.36874 ± 0.00019	12.9292 ± 0.0047	66.80 ± 0.14
T	[JD-2400000]	54716.80 ± 0.01	54712.62 ± 0.02	54699.42 ± 0.87	54603.0 ± 2.2
e		0 (fixed)	0 (fixed)	0.17 ± 0.07	0.38 ± 0.09
ω	[deg]	0 (fixed)	0 (fixed)	-110 ± 25	-33 ± 15
K	[m s^{-1}]	1.85 ± 0.23	12.48 ± 0.23	3.24 ± 0.24	2.63 ± 0.32
V	[km s^{-1}]		-9.2082 ± 0.0002		
$f(m)$	[$10^{-14} M_\odot$]	0.21	108.11	4.34	10.05
$m_2 \sin i$	[$M_\oplus$]	1.94	15.65	5.36	7.09
a	[AU]	0.03	0.04	0.07	0.22
N_{meas}			119		
$Span$	[days]		1570		
σ (O-C)	[ms^{-1}]		1.53		
χ^2_{red}			1.49		

measurements as a function of time (top panel), and the corresponding periodogram (lower panel). The figure suggests long term variations, over timescales of several thousands days which are much too long to be the rotational period. If those variation are real, they would be more likely to reflect an analog of 11 years solar magnetic cycle. Magnetic cycles can potentially affect apparent stellar velocities, since they can change the balance between ascending (blue-shifted) and receding (red-shifted) convective elements in the atmosphere, but we see no evidence for long-term RV variations. The other significant structure in the chromospheric signal is a broad power excess between 80 and 120 days, which is much more likely to reflect the rotation period. That peak overlapped our incorrect initial estimate of the period of GJ 581 d, but as discussed above photometry limits the amplitude of any velocity signal from spots at that period to at most a quarter of the observed value. The revised period puts a final nail in the coffin of that concern, since the periodogram of the Ca II H+K indices has no power excess around 67 days. The Ca II H + K periodogram finally has a weak peak at ∼ 15 days, which does not match any of the observed radial-velocity periods.

To summarize, none of the 4 periodic signal detected in our RV measurements is compatible with rotational modulation of stellar surface patterns. Four low-mass exoplanets orbiting the star remain, by far, the most likely interpretation.

6. Dynamical evolution

We reinvestigate the dynamics of the revised GJ 581 system, using the same techniques as in Beust et al. (2008, B08). With the SyMBA symplectic N-body code (Duncan et al. 1998), we carry 5-body integrations over 0.1 Gyr, with a 2×10^{-4} yr timestep. Starting from the nominal solutions (Tab.2), which assumes initially circular orbits for Gl581e and Gl581b (the two innermost planets), we perform those integrations for inclinations of 90 to 10 degrees, assuming full coplanarity of all orbits.

Our nominal simulation uses the periastron parameters derived in the Keplerian fit and listed in Table 1. To probe the sensitivity of the simulations to these parameters, we performed additional integrations with different starting values for the periastron longitudes. Unsurprisingly, since the orbits are non-resonant, the results were not significantly different.

Figure 4 shows the maximum variations of the semi-major axes and eccentricities during those integrations. As in B08, we note that the semi-major variations gradually increase as the inclination decreases. This is a clear indication that lower inclina-

tions, i.e. higher planetary masses, produce a less stable system. Compared to our previous study, the addition of GJ 581e drastically tightens the minimum inclination constraint. That low mass planet has little effect on the stability of the more massive GJ 581b, GJ 581c, and GJ 581d, but for inclinations $5 \leq i \leq 30°$, GJ 581e is ejected out of the system on time scales of at most a few Myrs.

The nominal integrations assume circular initial orbits for GJ 581e and GJ581b. Relaxing this constraint and setting the initial eccentricity of planet e to 0.1, we found the system even less stable: GJ 581e was then ejected for inclinations up to $i = 40°$.

Unlike most multi-planet radial-velocity systems, the nominal least square adjustment to the radial velocities is dynamically stable for sufficiently high inclinations (and co-planar orbits). Restricting the solutions to dynamically stable systems only imposes that $i \gtrsim 40°$ and therefore that the mass of each planet be no more than ∼1.6 times its minimum mass. For GJ 581e, b, c and d, those upper limits are 3.1, 30.4, 10.4 and 13.8 $M_\oplus$.

7. Summary and discussion

The large number of precise HARPS measurements has now revealed four planets in a non resonant-configuration. The false alarm probablities of all four planetary signals are below 0.01%. The orbital elements of planets GJ581b (P=5.36d Bonfils et al. 2005a) and GJ581c Udry et al. (P=12.9d 2007) are fully confirmed, and slightly refined. The 82 days Udry et al. (2007) period for GJ 581d, on the other hand, was a one-year alias of the true 66.8 days period of that planet. Our extended span and much larger number of measurements correct that confusion. Photometry, as well as monitoring of the Ca II H+K activity indicator over the four years of our spectroscopic measurements, indicate that the signal at 66 days does not originate in stellar activity. At the present time, and based on the well defined radial velocity signal and on an estimate of the worst-case effect of stellar activity, a planet with a period of 66.8 days is by far the most probable interpretation.

The new orbital elements for the outer planet GJ 581d correspond to a 0.22 AU semi-major axis. A planet with an eccentric orbit receives a larger orbit-averaged flux than a planet on a circular orbit of the same semi-major axis (Williams & Pollard 2002), and GJ 581 d receives the same average flux as a planet on a a = 0.21 AU circular orbit. The Udry et al. (2007) orbital elements of GJ 581d, with a 0.25 AU semi-major axis, located the planet close to the outer edge of the habitable zone, but most
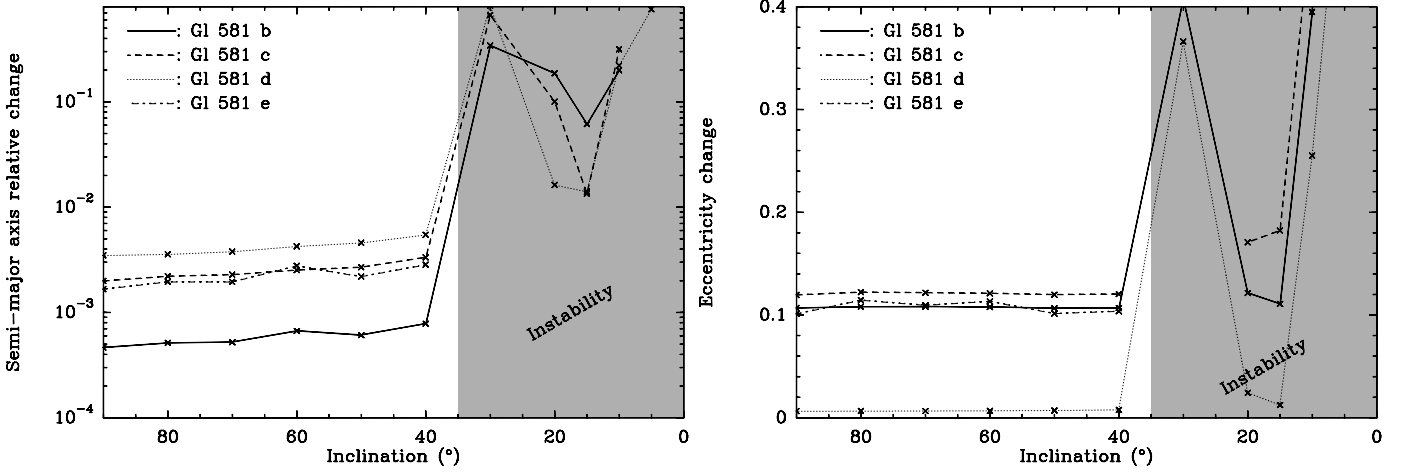
Fig. 4. Stability of various configurations of the four-planet Gl 581 system. The left and right panels respectively show the maximum variations, after $\times 10^8$ years, of the semi-major axes and of the eccentricities (right plot) as a function of the assumed inclination of the system (i=0 is pole-on). Each cross represents one simulation. The grey shading for $i < 35°$ marks an instable zone where one or more planets were ejected during the integration.

likely just slightly outside (e.g. Selsis et al. 2007). The revised parameters locate GJ 581d firmly in the habitable zone.

Thanks to 119 precise radial velocity measurements, we have discovered a fourth planets in the GJ 581 system. Its minimum mass, $m \sin i = 1.9 M_\oplus$, is by far the lowest amongst planets detected around main sequence stars. Such a low-mass planet is almost certainly rocky, and its equilibrium temperature is too high to allow a substantial atmosphere.

GJ 581 has the largest number of measurements in our HARPS M-star sample, which evidently helped detect such a low mass planet in a four planet system. The detection however does not stretch the limits of Doppler spectroscopy, and for the same period a planet only half as massive would have been detectable in our dataset. Our HARPS measurements set an upper limit of 1.2 m/s on the stellar jitter of GJ 581, based on a quadratic subtraction of just the mean photon noise from the observed dispersion of the radial-velocity residuals to the 4-planet solution. Some small fraction of this value could still be instrumental, but a 1.2 m/s "jitter" allows the detection of a 2 $M_\oplus$ planet with a 25 days orbital period. Such a planet would be earth-type and in the middle of the habitable zone of its M dwarf.

The stellar "jitter" has different physical components, with distinct time scales. For more massive stars and shorter integration times, acoustic modes represent a major contribution, but the short acoustic timescales in this small star and the 15 minutes integration ensure that they have been averaged out to below a few 0.1 m/s. The 1.2 m/s jitter therefore mostly reflects longer time-scale phenomena, such as granulation noise and changes in stellar surface anisotropies during a magnetic cycle. We are developing optimized measurement strategies to average out the granulation noise contribution to the stellar jitter, but HARPS already demonstrates that the global jitter (including instrumental errors, but not photon noise) of reasonably chromospherically quiet M dwarfs is at most of the order of 1 m/s.

This new low mass planet adds to the small set of Doppler-detected super-Earths, planets with a minimum mass under 10 $M_\oplus$. This planetary mass domain, as well as the Neptune-mass range ($<30 M_\oplus$) has largely been populated by the HARPS surveys. A few statistical properties have already emerged from these early discoveries (Mayor & Udry 2008):

– The full distribution of planetary masses is bimodal, with distinct peaks corresponding to gaseous giants and super-Earths. Despite the observational bias against low mass planets, the distribution below ~30 $M_\oplus$ rises towards super-Earth planets (cf. Fig. 7 in Mayor & Udry 2008).
– The majority of super-Earths and Neptunes are found in multiplanetary systems. Four of the 6 planetary systems with a known super-Earth, (GJ 876, HD 40307, HD 7924, GJ 176, GJ 581, HD 181433) have multiple planets. Two of these 4 multi-planet systems associate one super-Earth with one or two gaseous giant planets (GJ 876, HD 181433), and the other 2 have several low-mass planets on non resonant orbits (HD 40307, GJ 581). GJ 176 and HD 7924 have only one detected planet, though they could obviously have more which haven't been detected yet. GJ 176 is too magnetically active to easily detect a lower-mass planet, but the periodogram of HD 7924 does indeed show hints of possible additional planets (Howard et al. 2009).
– Contrary to gaseous giants, low mass planets seem no more frequent around metal-rich host stars (Udry et al. 2006).
– In a preliminary analysis, we have detected low mass close-in planets (P< 100d and $m \sin i < 30 M_\oplus$) around 30% of solar-type stars of the HARPS high precision survey (Lovis et al. 2009, in prep.).

Systems with several low mass close-in planets provide interesting constraints for models of planetary formation. Three systems are particularly noteworthy: HD 69830 (3 planets), HD 40307 (3 planets) and GJ 581 (4 planets).

Terquem & Papaloizou (2007), for instance, studied the migration of cores and terrestrial planets induced by their interaction with the protoplanetary disk, and suggest that "if hot super-Earths or Neptunes form by mergers of inwardly migrating cores, then such planets are most likely not isolated. We would expect to always find at least one, more likely a few, companions on close and often near-commensurable orbits". The high observed fraction of multi-planet systems matches that prediction, but the observed periods are quite far from near-commensurability.

Raymond et al. (2008) discuss observable consequences of planet formation models in systems with close-in terrestrial planets, and specifically address the case of GJ 581. In addition to

system architecture, they consider information from planet composition, which unfortunately is unavailable for the GJ 581 system. These authors find two formation mechanisms consistent with the available data: *in situ* formation, and formation at a larger distance followed by type I migration. *In situ* formation however would require a massive disk, 17-50 times above the minimum-mass disk. Type I migration from a larger distance, on the other hand, is expected to leave the close-in low mass planets in a MMR (mean motion resonance), at odds with the characteristics of the GJ 581 system.

Kennedy & Kenyon (2008) study hot super-Earths formation as a function of stellar mass and suggest that, with migration, short period low-mass planets are most likely to form around low-mass stars. Above approximately 1 solar-mass, the minimum protoplanet mass for migration to close-in orbits is above 10 Earth-masses and no hot super-Earths can form. Our searches for low mass planets with the HARPS spectrograph will test that prediction.

Zhou et al. 2009 (in prep.) study the birth of multiple super-Earths through sequential accretion. Focusing on the formation of the HD 40307 triple super-Earths system, they found evidence that massive embryos can assemble in a gaseous protostellar disk. The final states of their numerical simulations favor models with a reduction factor of ten for type I migration. These simulations quite succesfully reproduce the global structure of the triple super-Earth system, including non-resonant period ratios.

A very recent paper by Ogihara & Ida (2009) provides an illuminating discussion of formation mechanisms of low mass multiple planets orbiting M stars. It shows, in particular, that the final orbital configuration could be quite sensitive to migration timescale. The water fraction in low mass planets close to the habitable zone of M dwarfs is probably very large, making GJ 581d a serious candidate for an ocean planet (Léger et al. 2004).

Our HARPS surveys search for low-mass close-in planets around stars with masses from 0.3 to over 1 solar-mass. The numerous multiplanetary systems which they will detect will provide stimulating constraints for formation scenarios.

References

Bailey, J., Butler, R. P., Tinney, C. G., et al. 2009, ApJ, 690, 743
Beust, H., Bonfils, X., Delfosse, X., & Udry, S. 2008, A&A, 479, 277
Bonfils, X., Delfosse, X., Udry, S., Forveille, T., & Naef, D. 2006, in Tenth Anniversary of 51 Peg-b: Status of and prospects for hot Jupiter studies, ed. L. Arnold, F. Bouchy, & C. Moutou, 111–118
Bonfils, X., Delfosse, X., Udry, S., et al. 2005a, A&A, 442, 635
Bonfils, X., Forveille, T., Delfosse, X., et al. 2005b, A&A, 443, L15
Bonfils, X., Mayor, M., Delfosse, X., et al. 2007, A&A, 474, 293
Butler, R. P., Johnson, J. A., Marcy, G. W., et al. 2006, PASP, 118, 1685
Butler, R. P., Vogt, S. S., Marcy, G. W., et al. 2004, ApJ, 617, 580
Delfosse, X., Forveille, T., Mayor, M., et al. 1998, A&A, 338, L67
Duncan, M. J., Levison, H. F., & Lee, M. H. 1998, AJ, 116, 2067
Endl, M., Cochran, W. D., Kürster, M., et al. 2006, ApJ, 649, 436
Forveille, T., Bonfils, X., Delfosse, X., et al. 2009, A&A, 493, 645
Gilliland, R. L. & Baliunas, S. L. 1987, ApJ, 314, 766
Howard, A. W., Johnson, J. A., Marcy, G. W., et al. 2009, ApJ, 696, 75
Johnson, J. A., Butler, R. P., Marcy, G. W., et al. 2007, ApJ, 670, 833
Kennedy, G. M. & Kenyon, S. J. 2008, ApJ, 682, 1264
Kürster, M., Endl, M., Rouesnel, F., et al. 2003, A&A, 403, 1077
Léger, A., Selsis, F., Sotin, C., et al. 2004, Icarus, 169, 499
Lindegren, L. & Dravins, D. 2003, A&A, 401, 1185
Lovis, C., Mayor, M., Pepe, F., et al. 2006, Nature, 441, 305
Lovis, C. & Pepe, F. 2007, A&A, 468, 1115
Marcy, G. W., Butler, R. P., Fischer, D., et al. 2001, ApJ, 556, 296
Marcy, G. W., Butler, R. P., Vogt, S. S., Fischer, D., & Lissauer, J. J. 1998, ApJ, 505, L147
Mayor, M., Pepe, F., Queloz, D., et al. 2003, The Messenger, 114, 20
Mayor, M. & Udry, S. 2008, Physica Scripta Volume T, 130, 014010
Mayor, M., Udry, S., Lovis, C., et al. 2009, A&A, 493, 639
Ogihara, M. & Ida, S. 2009, astro-ph/0904.4543
Press, W. H., Teukolsky, S. A., Vetterling, W. T., & Flannery, B. P. 1992, Numerical recipes in C. The art of scientific computing (Cambridge: University Press, —c1992, 2nd ed.)
Queloz, D., Henry, G. W., Sivan, J. P., et al. 2001, A&A, 379, 279
Raymond, S. N., Barnes, R., & Mandell, A. M. 2008, MNRAS, 384, 663
Rivera, E. J., Lissauer, J. J., Butler, R. P., et al. 2005, ApJ, 634, 625
Saar, S. H. & Donahue, R. A. 1997, ApJ, 485, 319
Santos, N. C., Israelian, G., & Mayor, M. 2001, A&A, 373, 1019
Santos, N. C., Israelian, G., & Mayor, M. 2004, A&A, 415, 1153
Selsis, F., Kasting, J. F., Levrard, B., et al. 2007, A&A, 476, 1373
Terquem, C. & Papaloizou, J. C. B. 2007, ApJ, 654, 1110
Udry, S., Bonfils, X., Delfosse, X., et al. 2007, A&A, 469, L43
Udry, S., Mayor, M., Benz, W., et al. 2006, A&A, 447, 361
von Bloh, W., Bounama, C., Cuntz, M., & Franck, S. 2007, A&A, 476, 1365
Williams, D. M. & Pollard, D. 2002, International Journal of Astrobiology, 1, 61
Zechmeister, M. & Kürster, M. 2009, A&A, 496, 577
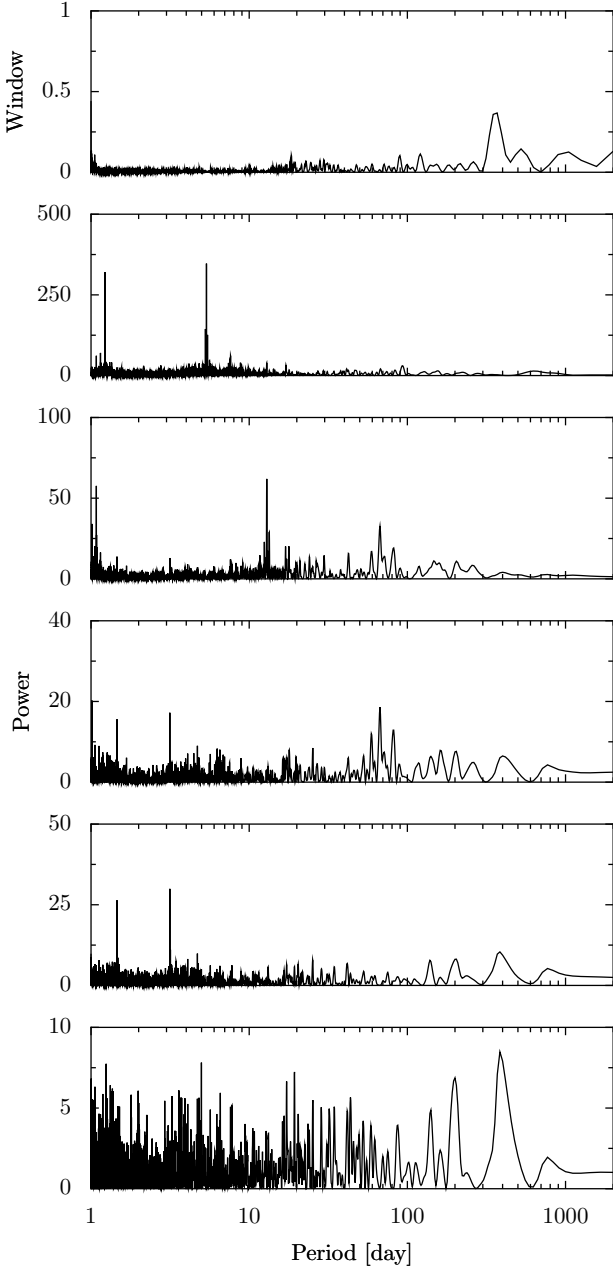
Fig. 1. Periodograms of GJ581 radial velocity measurements. *Panel 1 (top)*: Window function of the HARPS measurements. *Panel 2*: Periodogram of the HARPS velocities. The peaks corresponding to GJ581b (P=5.36d) and its alias with one sidereal day are clearly visible. *Panel 3*: HARPS velocities corrected from the velocity variation due to GJ581b. The peak corresponding to GJ581c (P=12.9d) appears. *Panel 4*: Removing the variability due to planets b and c, we can see the peak due to the P=3.15d variability of GJ581e (+ the alias with the a one sideral day period) as well as the peak at 66d due to GJ581d. *Panel 5*: Periodogram after removing the effect of planets b, c and d. The peak due to planet e (Mass = 1.9 earth-mass) is evident (+ its one-day aliases). *Panel 6 (bottom)*: Removing the velocity wobbles due to the four planets, the periodogram of the residual velocities shows no additional significant peaks.
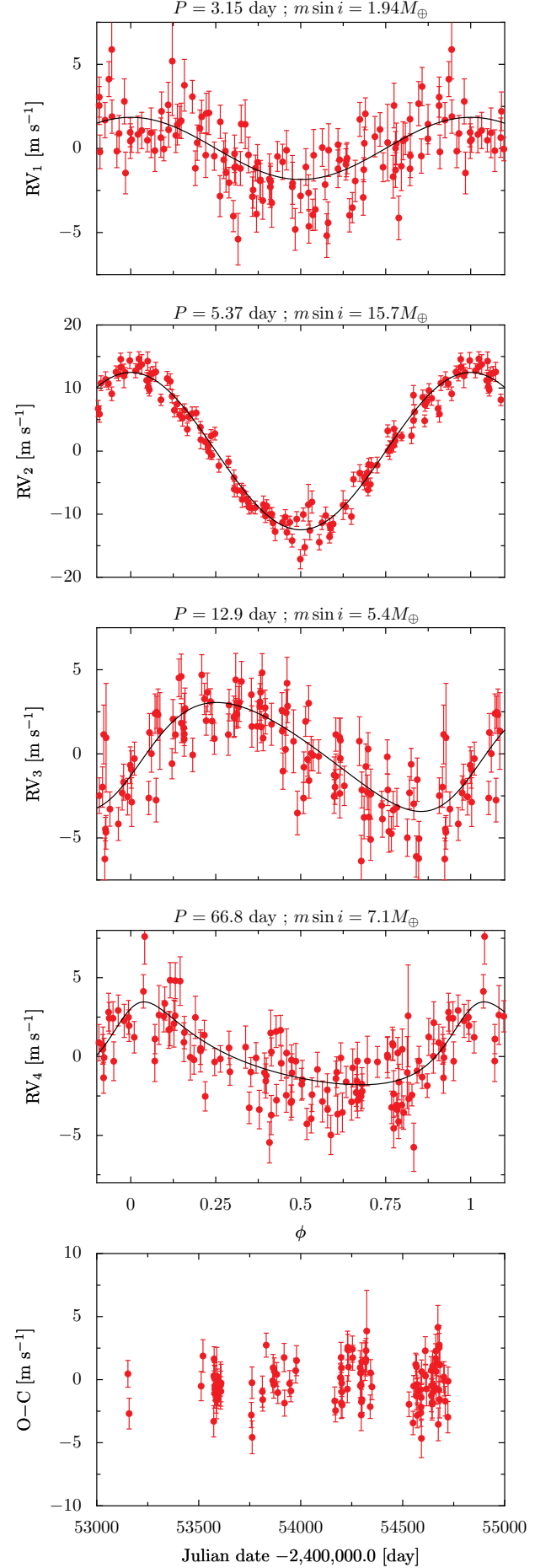
Fig. 2. Radial velocity curves for planets e, b, c and d, from top to bottom. The lowest panel displays the residual to the four-planets keplerian fit.
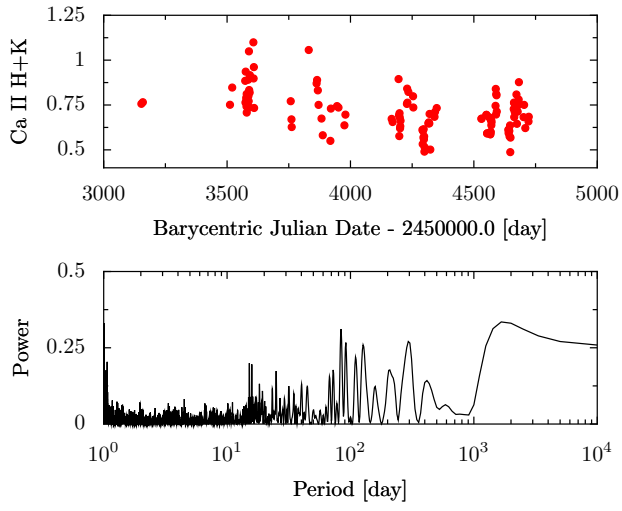
Fig. 3. The Ca II H+K index as function of Julian date (upper panel) and its periodogram (lower panel).

Table 1. Radial-velocity measurements, associated uncertainties and Ca II H+K index for Gl581. All radial velocities are relative to the solar system barycenter (and not corrected from the 0.20 m s^{-1} perspective acceleration of GJ 581). Only available electronically.

JD-2400000	RV [km s^{-1}]	Uncertainty [km s^{-1}]	Ca II H+K
53152.712894	-9.21879	0.0011	0.751
53158.663460	-9.22730	0.0012	0.847
53511.773341	-9.21549	0.0012	0.885
53520.744746	-9.19866	0.0013	0.764
53573.512039	-9.20874	0.0012	0.936
53574.522329	-9.19922	0.0011	0.766
53575.480749	-9.20466	0.0010	0.790
53576.536046	-9.21536	0.0010	0.775
53577.592603	-9.21927	0.0012	0.742
53578.510713	-9.20889	0.0009	0.812
53578.629602	-9.20628	0.0011	0.708
53579.462557	-9.19585	0.0009	0.891
53579.621049	-9.19414	0.0010	0.800
53585.461770	-9.20243	0.0010	0.771
53586.465158	-9.21196	0.0007	1.049
53587.464704	-9.22556	0.0014	0.833
53588.538062	-9.21678	0.0023	0.736
53589.462024	-9.20322	0.0007	0.819
53590.463895	-9.19562	0.0008	0.916
53591.466484	-9.20138	0.0007	1.099
53592.464813	-9.21424	0.0008	0.898
53606.551679	-9.19397	0.0019	0.961
53607.507527	-9.19849	0.0010	0.733
53608.482643	-9.21273	0.0012	0.771
53609.488452	-9.22225	0.0015	0.670
53757.877319	-9.20435	0.0010	0.627
53760.875475	-9.21109	0.0013	1.057
53761.859216	-9.20177	0.0013	0.870
53811.846943	-9.20333	0.0012	0.889
53813.827017	-9.21874	0.0009	0.832
53830.836957	-9.21013	0.0009	0.751
53862.701441	-9.20862	0.0009	0.674
53864.713662	-9.19447	0.0010	0.581
53867.752171	-9.21747	0.0011	0.550
53870.696603	-9.20299	0.0011	0.730
53882.657763	-9.21956	0.0009	0.744
53887.690738	-9.21332	0.0009	0.736
53918.621751	-9.20079	0.0011	0.637
53920.594947	-9.22608	0.0010	0.696
53945.543122	-9.19820	0.0010	0.673
53951.485927	-9.20254	0.0009	0.655
53975.471596	-9.21567	0.0010	0.895
53979.543975	-9.21606	0.0012	0.693
54166.874182	-9.22284	0.0011	0.577
54170.853961	-9.20059	0.0009	0.704
54194.872349	-9.22170	0.0011	0.681
54196.750384	-9.19345	0.0012	0.620
54197.845039	-9.19264	0.0012	0.631
54198.855509	-9.21129	0.0012	0.662
54199.732869	-9.21393	0.0010	0.756
54200.910915	-9.20829	0.0010	0.841
54201.868554	-9.19897	0.0010	0.763
54202.882595	-9.19475	0.0010	0.823
54228.741561	-9.19964	0.0011	0.799
54229.700478	-9.19722	0.0014	0.736
54230.762136	-9.20982	0.0010	0.612
54234.645916	-9.19421	0.0011	0.532
54253.633168	-9.21733	0.0010	0.605
54254.664810	-9.21238	0.0010	0.569

Table 1. continued.

JD-2400000	RV [km s^{-1}]	Uncertainty [km s^{-1}]	Ca II H+K
54291.568850	-9.21520	0.0013	0.615
54292.590814	-9.20807	0.0009	0.558
54293.625868	-9.19804	0.0010	0.575
54295.639448	-9.21852	0.0011	0.490
54296.606114	-9.22915	0.0012	0.515
54297.641939	-9.21556	0.0010	0.647
54298.567600	-9.20023	0.0011	0.653
54299.622195	-9.19742	0.0015	0.647
54300.619110	-9.20792	0.0010	0.700
54315.507494	-9.19471	0.0016	0.501
54317.480847	-9.21647	0.0010	0.684
54319.490527	-9.20583	0.0013	0.711
54320.544072	-9.19620	0.0010	0.733
54323.507050	-9.21928	0.0032	0.674
54340.555781	-9.20957	0.0009	0.695
54342.486204	-9.18958	0.0010	0.592
54349.515163	-9.21982	0.0010	0.680
54530.855660	-9.20187	0.0010	0.587
54550.831274	-9.20188	0.0009	0.600
54553.803722	-9.22133	0.0008	0.666
54563.838002	-9.21136	0.0009	0.674
54566.761147	-9.20787	0.0011	0.695
54567.791671	-9.19972	0.0010	0.592
54569.793302	-9.22225	0.0010	0.680
54570.804248	-9.22375	0.0010	0.587
54571.818376	-9.20449	0.0011	0.600
54587.861968	-9.20505	0.0015	0.666
54588.838799	-9.19985	0.0011	0.637
54589.827493	-9.20286	0.0011	0.655
54590.819634	-9.21398	0.0010	0.745
54591.817120	-9.22848	0.0015	0.840
54592.827337	-9.21685	0.0009	0.697
54610.742932	-9.18919	0.0011	0.811
54611.713477	-9.19994	0.0009	0.804
54616.713028	-9.19947	0.0013	0.713
54639.686739	-9.21881	0.0011	0.611
54640.654409	-9.21858	0.0013	0.594
54641.631706	-9.20599	0.0010	0.614
54643.644998	-9.20581	0.0013	0.605
54644.587028	-9.21830	0.0012	0.575
54646.625357	-9.21515	0.0012	0.636
54647.579119	-9.20087	0.0011	0.487
54648.484817	-9.19842	0.0011	0.568
54661.553706	-9.22001	0.0012	0.728
54662.549408	-9.20873	0.0013	0.763
54663.544866	-9.19438	0.0011	0.683
54664.553042	-9.19450	0.0012	0.759
54665.569376	-9.20207	0.0010	0.712
54672.531723	-9.21359	0.0018	0.809
54674.524120	-9.19858	0.0013	0.645
54677.505114	-9.21696	0.0011	0.713
54678.556785	-9.20646	0.0011	0.748
54679.504034	-9.19434	0.0015	0.770
54681.514143	-9.20461	0.0014	0.781
54682.503343	-9.21537	0.0013	0.877
54701.485074	-9.19390	0.0012	0.682
54703.513042	-9.21009	0.0012	0.751
54708.479050	-9.21261	0.0012	0.621
54721.473033	-9.22361	0.0012	0.658
54722.472371	-9.20543	0.0011	0.684